Experimental Evaluation of Predictive Combustion Phasing Control in an HCCI Engine using Fast Thermal Management and VVA

Widd, Anders; Ekholm, Kent; Tunestål, Per; Johansson, Rolf

Published in:
Proceedings of the IEEE International Conference on Control Applications

DOI:
10.1109/CCA.2009.5281087

2009

18th IEEE International Conference on Control Applications
Part of 2009 IEEE Multi-conference on Systems and Control
Saint Petersburg, Russia, July 8-10, 2009

Experimental Evaluation of Predictive Combustion Phasing Control in an HCCI Engine using Fast Thermal Management and VVA

Anders Widd, Kent Ekholm, Per Tunestål, and Rolf Johansson

Abstract— **This paper presents experimental results on model predictive control of the combustion phasing in a Homogeneous Charge Compression Ignition (HCCI) engine. The controllers were based on linearizations of a previously presented physical model of HCCI including cylinder wall temperature dynamics. The control signals were the inlet air temperature and the inlet valve closing. A system for fast thermal management was installed and controlled using mid-ranging control. The resulting control performance was experimentally evaluated in terms of response time and steady-state output variance. For a given operating point, a comparable decrease in steady-state output variance was obtained either by introducing a disturbance model or by changing linearization point. The robustness towards disturbances was investigated as well as the effects of varying the prediction and control horizons.**

I. INTRODUCTION

Homogeneous Charge Compression Ignition (HCCI), also referred to as Controlled Auto-Ignition (CAI), holds promise for reduced emissions and increased efficiency compared to conventional internal combustion engines. As HCCI lacks direct actuation over the combustion phasing, much work has been devoted to designing controllers capable of set-point tracking and disturbance rejection. Ignition timing in HCCI engines is determined by several factors [1] including the auto-ignition properties of the air-fuel mixture, the intake temperature, the amount of residual gases in the cylinder, etc. As a consequence, there are many possible choices of control signals, such as [1] variable valve timing, intake temperature, and the amount of residuals trapped in the cylinder.

The control results presented in this paper were obtained using a cycle-resolved physical model. Model Predictive Control (MPC) [2] was used with the crank angle of inlet valve closing, θ_{IVC}, and the intake temperature, T_{in}, as control signals. The controlled output was the crank angle of 50% burned, θ_{50}. The results were evaluated in terms of response time, robustness towards disturbances, and combustion phasing variance, extending the experimental investigation of the closed-loop properties [3], [4]. A fast response to combustion phasing set-point changes can be critical to avoid—e.g., misfire or too high peak pressures during certain load changes. To this purpose, our focus was on the steady-state output variance. Recent examples of cycle-resolved models of HCCI for control design include [5], [6], where [6] also presented experimental results of closed-loop control. Continuous-time models including cylinder wall temperature models were presented in [7], [8]. The latter synthesized an LQ controller using a cycle-resolved statistical version of the model and presented experimental results. Fast thermal management and variable compression ratio was employed in [9] using several control methods. Model predictive control of HCCI engines based on statistical models was used in [10].

A review of the model is given in Sec. II. In Sec. III, the mid-ranging strategy for the intake temperature and the predictive control of θ_{50} are described. The experimental set-up is described in Sec. IV and experimental results are presented in Sec. V. The paper ends with a discussion in Sec. VI, followed by conclusions.

A. Widd and R. Johansson are with the Department of Automatic Control, Lund University, Box 118 SE 221 00 Lund, Sweden. {Anders.Widd | Rolf.Johansson}@control.lth.se

K. Ekholm and P. Tunestål are with the Division of Combustion Engines, Department of Energy Sciences, Lund University, Box 118 SE 221 00 Lund, Sweden. {Kent.Ekholm | Per.Tunestal}@energy.lth.se

II. MODELING

For more details on the nonlinear model, see [3], [4]. It uses the same basic formulation as [6] with the inclusion of cylinder wall temperature dynamics and a few modifications.

A. Cylinder Wall Temperature Dynamics

The cylinder wall was modeled as a single mass with a slowly varying outer surface temperature T_c, a convective flow $\dot{q}_a$ between the in-cylinder gases and the cylinder wall, and a conductive flow $\dot{q}_b$ through the wall, see Fig. 1. The first law of thermodynamics applied to the gas when no work is performed yields the expression $\dot{T} = -\dot{q}_a/mC_v$ where T, m, and C_v are the temperature, mass, and specific heat of the gas. The Newton law $\dot{q}_a = h_c A_c(T - T_w)$ was applied, where h_c is the convection coefficient, A_c is the wall surface area and T_w is the wall surface temperature. The time derivative of the inner wall temperature, T_{iw}, is given by $\dot{T}_{iw} = (\dot{q}_a - \dot{q}_b)/m_c C_p$ where C_p is the specific heat of the cylinder wall, and m_c is the cylinder wall mass. The conductive flow is given by $\dot{q}_b = (T_w - T_c)k_c A_c/L_c$ where k_c is the conduction coefficient and L_c is the wall thickness. Assuming that the steady-state temperature condition $T_{iw} = (T_w + T_c)/2$ holds the temperature equations may be written as

$$\dot{\mathcal{T}} = A_{ht}\mathcal{T} + B_{ht}T_c, \tag{1a}$$

$$A_{ht} = \begin{bmatrix} -\frac{h_c A_c}{mC_v} & \frac{h_c A_c}{mC_v} \\ 2\frac{h_c A_c}{m_c C_p} & -2\frac{h_c A_c + k_c A_c/L_c}{m_c C_p} \end{bmatrix}, \tag{1b}$$

$$B_{ht} = \begin{bmatrix} 0 \\ 2\frac{k_c A_c}{L_c m_c C_p} \end{bmatrix}, \quad \mathcal{T} = \begin{bmatrix} T \\ T_w \end{bmatrix} \tag{1c}$$

Since T_c is assumed to be slowly varying, it can be assumed constant over a short time t_i. The temperature state at t_i,

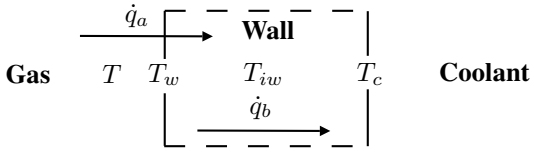

Fig. 1. Principle of the cylinder wall model.

given an initial state $\mathcal{T}(0)$, can then be computed as

$$\mathcal{T}(t_i) = \Phi_i \mathcal{T}(0) + \Gamma_i T_c \quad (2)$$

$$\Phi_i = e^{A_{ht} t_i}, \quad \Gamma_i = \int_0^{t_i} e^{A_{ht}(t_i-\tau)} B_{ht} d\tau \quad (3)$$

Eq. (2) was used to update the gas temperature and the wall temperature after mixing, after combustion, and after expansion to capture the time constant of the cylinder wall temperature while keeping the complexity at a tractable level. Since the integration time t_i had to be adapted to each instant and some of the parameters depend on the in-cylinder state, three sets of matrices $\{\Phi_i, \Gamma_i\}$, $i = 1, 3, 5$ were used, where $i = 1$ corresponded to mixing; $i = 3$ combustion; $i = 5$ expansion. The cylinder wall temperature was assumed constant between the heat transfer events.

B. Temperature Trace

Throughout the cycle, isentropic expansion and compression was assumed, with definitions from [11].

Definition 1: The temperature T_B and pressure P_B after isentropic compression or expansion from volume V_A to volume V_B with initial temperature and pressure T_A and P_A are given by

$$T_B = T_A \left(\frac{V_A}{V_B}\right)^{\gamma-1}, \quad P_B = P_A \left(\frac{V_A}{V_B}\right)^{\gamma} \quad (4)$$

where γ is the specific heat ratio.

Definition 2: The temperature T_B after isentropic compression or expansion from pressure P_A to P_B is

$$T_B = T_A \left(\frac{P_B}{P_A}\right)^{(\gamma-1)/\gamma} \quad (5)$$

1) Intake/Mixing: The gas temperature at the start of cycle k, $T_1(k)$, was modeled as a weighted average of the temperatures of the intake and the trapped residuals, cf. [6];

$$T_1(k) = \frac{C_{v,in} T_{in}(k) + C_{v,EGR} \chi \alpha T_{5+}(k-1)}{C_{v,in} + \alpha C_{v,EGR}}, \quad (6)$$

where $C_{v,in}$ and $C_{v,EGR}$ are the specific heats of the fresh reactants and the residual gases respectively and α is the molar ratio between trapped residuals and inducted gases. The final gas temperature of cycle $k-1$ is denoted $T_{5+}(k-1)$, and χ is a measure of how much the residual temperature has decreased. The initial wall temperature of cycle k was set equal to the final wall temperature of cycle $k-1$;

$$T_{w1}(k) = T_{w5+}(k-1) \quad (7)$$

Eq. (2) with $i = 1$ was applied to yield new temperatures $T_{1+}(k)$ and $T_{w1+}(k)$;

$$\begin{bmatrix} T_{1+}(k) \\ T_{w1+}(k) \end{bmatrix} = \Phi_1 \begin{bmatrix} T_1(k) \\ T_{w1}(k) \end{bmatrix} + \Gamma_1 T_c \quad (8)$$

2) Compression: Isentropic compression from the volume at inlet valve closing, $V_1(k)$, to the volume at auto-ignition, $V_2(k)$, was assumed, yielding temperature $T_2(k)$ and pressure $P_2(k)$.

3) Auto-Ignition: The crank angle of auto-ignition, $\theta_{\text{ign}}(k)$, was modeled as in [12], so that the condition

$$\int_{\theta_{\text{IVC}}(k)}^{\theta_{\text{ign}}(k)} f_k(\theta) d\theta = 1 \quad (9)$$

was fulfilled with

$$f_k(\theta) = A_a P_{in}^n \mathcal{V}_k(\theta)^{\gamma n} \exp\left(-\frac{E_a \mathcal{V}_k(\theta)^{1-\gamma}}{R T_{1+}(k)}\right) \quad (10)$$

The parameter A_a is a scaling factor, E_a is the activation energy for the reaction, n is the reaction sensitivity to pressure, R is the gas constant, and $\mathcal{V}_k(\theta) = V_1(k)/V(\theta)$. Note that the integrand is independent of species concentrations. To obtain an explicit expression for θ_{ign}, an approach similar to [6] was taken. The integrand was approximated with its maximum value, which is attained at Top Dead Center (TDC). The corresponding crank angle degree (CAD) was denoted θ_{TDC}, so that $f_k(\theta) = f_k(\theta_{\text{TDC}})$. The lower integration limit was then shifted from θ_{IVC} to θ_{TDC} and the resulting integral equation was solved for $\theta_{\text{ign}}(k)$;

$$\theta_{\text{ign}}(k) = \Delta\theta_A + \frac{1}{f_k(\theta_{\text{TDC}})} \quad (11)$$

where $\Delta\theta_A$ is an offset in CAD.

4) Combustion: The temperature after combustion was calculated as

$$T_3(k) = T_2(k) + \frac{Q_{LHV}}{(1+\alpha)(\phi^{-1}(m_a/m_f)_s + 1) C_v} \quad (12)$$

where Q_{LHV} is the lower heating value of the fuel, ϕ is the equivalence ratio, and $(m_a/m_f)_s$ is the stoichiometric air-to-fuel ratio. The denominator approximates the ratio between the total in-cylinder mass and the fuel mass [3]. Eq. (2) was applied with $i = 3$ and $T_{w3}(k) = T_{w1+}(k)$ to find new temperatures $T_{3+}(k)$, $T_{w3+}(k)$. The pressure after combustion is then

$$P_3(k) = \frac{T_{3+}(k)}{T_2(k)} P_2(k) \quad (13)$$

5) Expansion: The gas temperature and pressure after expansion, $T_4(k)$ and $P_4(k)$, were calculated assuming adiabatic expansion from $V_2(k)$ to the volume at exhaust valve opening, $V_4(k)$. At exhaust valve opening isentropic expansion from the in-cylinder pressure to atmospheric pressure was assumed, yielding temperature $T_5(k)$. Finally, Eq. (2) was applied with $i = 5$ and $T_{w5}(k) = T_{w3+}(k)$ to obtain the final gas temperature $T_{5+}(k)$ and the final wall temperature $T_{w5+}(k)$.

C. Model Outputs

The combustion duration is a function of the charge temperature, composition, and θ_{ign} [12]. Around an operating point the combustion duration was assumed constant, yielding the following expression for θ_{50}, where $\Delta\theta$ is an offset in crank angle degrees.

$$\theta_{50}(k) = \theta_{ign}(k) + \Delta\theta \tag{14}$$

The indicated mean effective pressure (IMEP_n) was calculated from the gas temperatures [11];

$$\text{IMEP}_n(k) = \frac{mC_v}{V_d}\left(T_{1+}(k) - T_2(k) + T_{3+}(k) - T_4(k)\right) \tag{15}$$

where V_d is the displacement volume.

D. State Selection and Linearization

Using (2), (10), (11), (12), (14), (15), and the assumption of isentropic compression and expansion, the temperature state can be uniquely determined from the outputs [4]. This makes it possible to have IMEP_n and θ_{50} as states. Both quantities can be obtained from in-cylinder pressure measurements. The model then takes the following form.

$$x(k+1) = \mathbf{F}(x(k), u(k)) \tag{16}$$

$$x(k) = \begin{bmatrix}\text{IMEP}_n(k)\\ \theta_{50}(k)\end{bmatrix}, \quad u(k) = \begin{bmatrix}\theta_{\text{IVC}}(k)\\ T_{\text{in}}(k)\end{bmatrix} \tag{17}$$

The function $\mathbf{F}(x(k), u(k))$ is parametrized by the amount of injected fuel, the amount of recycled exhaust gases (EGR), the intake pressure, etc. [4]. Fig. 2 shows calibration results originally presented in [3]. The nonlinear model was run in open loop and measurements of θ_{50}, IMEP_n, and the wall temperature T_w were available. Around cycle index 200 the amount of injected fuel was increased. The model captures the qualitative and quantitative behaviour of the three outputs. The symbolic toolbox in MATLAB was used

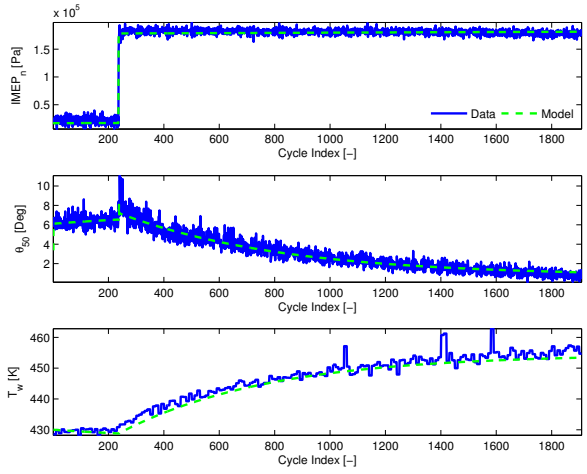

Fig. 2. IMEP_n, θ_{50}, and T_w measured and model output during a step in equivalence ratio. Figure reproduced from [3].

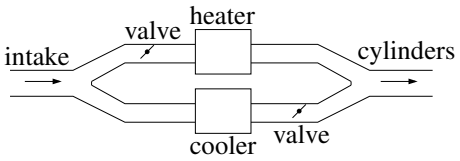

Fig. 3. Schematic of the fast intake temperature control system.

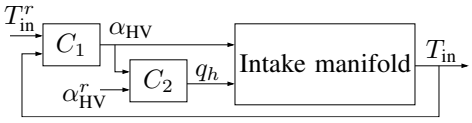

Fig. 4. Intake temperature control strategy.

to obtain linearizations according to

$$x(k+1) = Ax(k) + Bu(k) \tag{18}$$

$$y(k) = x(k) \tag{19}$$

$$A = \frac{\partial x(k+1)}{\partial x(k)}(x^0, u^0), \quad B = \frac{\partial x(k+1)}{\partial u(k)}(x^0, u^0)$$

where (x^0, u^0) is a stationary operating point.

III. CONTROL DESIGN

A. Intake Temperature Control

The intake temperature was governed by two valves, a cooler, and a heater, see Fig. 3. A similar system was used in [9] and there denoted Fast Thermal Management. The heater power (q_h) could be set as well as the positions of the two valves, denoted α_{HV} and α_{CV} for the heater valve and the cooler valve respectively.

1) Control Strategy: Assuming that the conditions before and after the throttles are approximately equal, the mass flow and pressure after the throttles can be maintained by requiring that the total projected flow area of the two throttles is kept constant. This assumption is not likely to hold for the individual throttles, but the experiments suggest that the impact on the resulting intake pressure is small. Denote by $\bar{A}_{\text{th}}$ the areas of each throttle plate. The projected flow area of each plate is then given by

$$A_{\text{HV}} = (1 - \cos\alpha_{HV})\,\bar{A}_{\text{th}}, \quad A_{\text{CV}} = (1 - \cos\alpha_{CV})\,\bar{A}_{\text{th}} \tag{20}$$

The condition of constant projected flow area can be written $\bar{A}_{\text{th}} = A_{\text{HV}} + A_{\text{CV}}$ and solving for α_{CV} gives

$$\alpha_{\text{CV}} = \cos^{-1}(1 - \cos(\alpha_{\text{HV}})) \tag{21}$$

With this relation between α_{HV} and α_{CV} the intake temperature control system has two inputs (α_{HV} and q_h) and one output (T_{in}). The heater input is relatively slow while the valve has a faster response but a narrower operating range, making the system suitable for mid-ranging control [13]. An example of HCCI control using a mid-ranging strategy was presented in [14]. A block diagram of the mid-ranging intake temperature control strategy is shown in Fig. 4. Controller C_1 governed α_{HV} to fulfill $T_{in} = T_{in}^r$ where T_{in}^r is the desired intake temperature. Controller C_2 governed q_h in order to keep α_{HV} at a desired value α_{HV}^r. Choosing α_{HV}^r slightly above the middle of the operating range gave a fairly fast

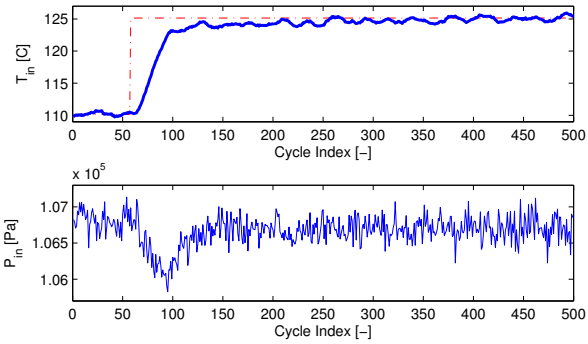

Fig. 5. Intake temperature control, closed-loop step response. The bottom plot shows the intake pressure.

response to changes in the desired intake temperature (Fig. 5), cf. [4]. The intake pressure is also shown in Fig. 5, the variation during the step is less than one percent. A lower bound on α_{HV} greater than zero was introduced in order to always maintain a minimum hot flow to avoid damages to the heater.

B. Predictive Control of Combustion Phasing

Model predictive control was shown to be a suitable control strategy for HCCI [15] due to its MIMO-capabilities and its ability to handle explicit constraints on control signals and outputs. In [10] similar closed-loop performance was demonstrated using MPC, LQ, and PID controllers in certain operating conditions. From a tuning perspective, however, the ability to enforce explicit constraints on the control signals using MPC, is advantageous [2]. Consider the cost function

$$J(k) = \sum_{i=1}^{H_p} \mathcal{Y}(i|k) + \sum_{i=0}^{H_u-1} \mathcal{U}(i|k) \quad (22)$$

$$\mathcal{Y}(i|k) = ||\hat{y}(k+i|k) - r(k+i|k)||_Q^2, \quad (23)$$

$$\mathcal{U}(i|k) = ||\Delta\hat{u}(k+i|k)||_R^2 \quad (24)$$

where $\hat{y}(k+i|k)$ is the predicted output at time $k+i$ given a measurement at time k, $\Delta\hat{u}(k+1|k)$ is the predicted change in control signal, and $r(k+i|k)$ is the reference value at time $k+i$. The parameters H_p and H_u define the length of the prediction horizon and the control horizon. At each sample, the cost function in (22) is minimized by determining a sequence of changes to the control signal $\Delta u(k+i|k)$, $i = 0 \dots H_u - 1$, subject to the constraints

$$y_{min} \leq y(k) \leq y_{max} \quad (25)$$

$$u_{min} \leq u(k) \leq u_{max} \quad (26)$$

$$\Delta u_{min} \leq \Delta u(k) \leq \Delta u_{max} \quad (27)$$

for all k. The first step of the optimal sequence is then applied to the plant and the optimization is repeated in the next step yielding a new optimal sequence [2].

1) Controller Tuning: The linear model in (18) was used to generate predictions. As only control of θ_{50} was the control objective, there was no penalty on IMEP$_n$, but it was used as a measurement. A small weight was added to penalize $\theta_{\text{IVC}} - \theta_{\text{IVC}}^r$, where θ_{IVC}^r is a set-point for the control signal, to obtain a slight mid-ranging effect as there are several combinations of control signals that achieve the same output. To avoid excitation effects related to the gas exchange, θ_{IVC} was restricted to $\theta_{\text{IVC}} \in [550, 620]$. The inlet temperature was restricted to $T_{\text{in}} \in [110, 135]$. To obtain error-free tracking, a disturbance observer [16] was used.

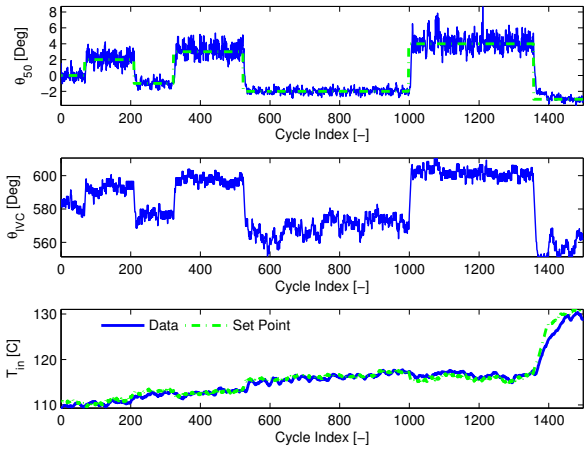

Fig. 6. Response to steps of increasing amplitude. All set-point changes are accomplished within 20 cycles.

IV. Experimental Setup

The experimental setup was described in [14]. The experiments were performed on a six-cylinder heavy-duty Volvo diesel engine, also used in [10], [17]. The engine had a 2000 cm^3 displacement volume, a 131 mm stroke, and a 150 mm bore. The connecting rod length was 260 mm and the compression ratio was 18.5:1. Ethanol was port injected. Due to technical circumstances, four of the six cylinders (Cylinder 1, 3, 5, and 6) were operated. The inlet valve closing of each cylinder was governed by four identical controllers while the intake temperature was governed only by Cylinder 5. The main focus was on this cylinder, some multi-cylinder results are presented in Sec. V-D. The control system was run on a Linux PC with a 2.4 GHz Intel Pentium 4 processor, see [14]. The experiments were performed at an engine speed of 1200 rpm, yielding a sample time of 0.1 seconds per cycle. The midranging control strategy for T_{in} was implemented in C++ while the predictive controllers were implemented in Simulink and compiled using Real-Time Workshop. The injected fuel energy was 1400 J and no exhausts were recycled, yielding approximately 3.5 bar IMEP$_n$ in all experiments. When evaluating the robustness towards disturbances the engine speed, the fuel energy, and the amount of recycled exhaust gases were varied.

V. Experimental Results

A typical response to a sequence of steps with increasing amplitude is shown in Fig. 6. The response time was less than 20 cycles for all steps. The intake temperature changed only slightly until the final step, where the inlet valve reached a constraint.

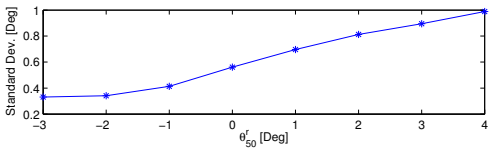

Fig. 7. Output standard deviation plotted against the set-point for θ_{50}.

A. Statistical Properties

As seen in Fig. 6, the output variance increased notably with later combustion phasing. Fig. 7 shows the steady-state output standard deviation plotted against the θ_{50}-reference.

1) Disturbance Modeling: In an attempt to reduce the steady-state output variance at the later combustion phasing, a disturbance model was identified. The model residuals were formed as

$$e_m(k) = \theta_{50}(k) - \hat{\theta}_{50}(k) \tag{28}$$

where $\hat{\theta}_{50}(k)$ is the output of the linearized model in response to the input signals. A stochastic realization was found using a subspace-based algorithm [18]. There was a distinct gap in magnitude after the first singular value of the identified subspace, indicating that a first-order model was sufficient. A model on the following form was obtained

$$e_x(k+1) = ae_x(k) + Kv(k) \tag{29a}$$
$$e_m(k) = Ce_x(k) + v(k) \tag{29b}$$

where e_x is the state and $v(k) \in \mathcal{N}(0, R_e)$.

2) Extended Controller: The model in (18) was extended with the disturbance model in (29). A controller was designed based on the extended model using the same design parameters as for the nominal controller. For set-points close to $\theta^r_{50} = 0$ there was no significant reduction in the output variance. However, for $\theta^r_{50} = 4$ the output variance was reduced by almost 10%.

B. Robustness Towards Disturbances

The robustness towards disturbances in the amount of fuel, the engine speed, and the amount of recycled exhaust gases was investigated experimentally. Fig. 8 shows the response as disturbances were added sequentially. At cycle 200 the engine speed was increased from 1200 rpm to 1400 rpm. The injected fuel energy was reduced from 1400 J to 1200 J at cycle 700. Finally, the amount of recycled exhaust gases (EGR) was increased from approximately 0% to 30% at cycle 1350. The bottom plot shows IMEP_n which reflects the impact of the disturbances in engine speed and fuel energy. The combustion phasing was maintained relatively well through the whole sequence.

C. Prediction Horizons

A prediction horizon of 5 and a control horizon of 2 was used in the nominal controller. The effects of increasing the horizons were evaluated in terms of control performance and computation time for each cycle. Table I shows the average computation time measured in processor clock cycles normalized by the nominal average. As expected, the computation time grows mainly with the choice of control horizon. The most demanding setting tested, $H_p = 30$, $H_u = 15$, has

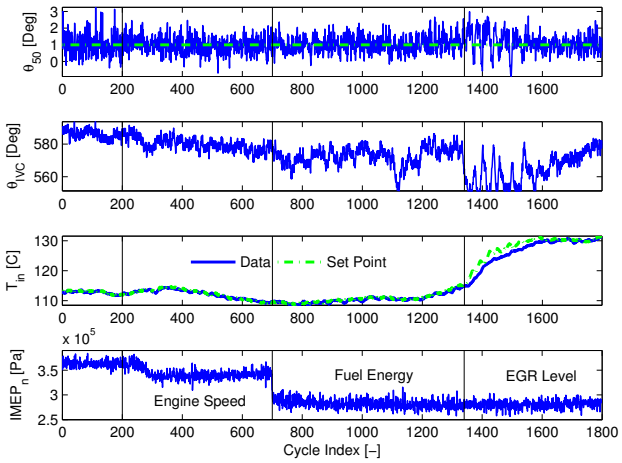

Fig. 8. Response to disturbances in the engine speed, the amount of injected fuel, and the amount of EGR. IMEP_n is included to visualize the disturbances in engine speed and fuel energy.

TABLE I

COMP. TIME FOR DIFFERENT PREDICTION AND CONTROL HORIZONS.

H_p	H_u	CPU Cycles (relative)
5	2	1.0000
10	2	1.0059
10	4	2.6000
15	6	5.8647
15	8	13.3294
20	10	26.0412
30	15	58.8235

a computation time almost sixty times longer than that of $H_p = 5$, $H_u = 2$. However, in terms of control results, the controllers performed practically identically both in terms of response time and output variance.

D. Multi-Cylinder Control

As previously mentioned, four of the cylinders were operated and the controller for Cylinder 5 governed the intake temperature. During a series of step changes in the set-point for θ_{50} the θ_{IVC}-values requested by the controllers showed a large spread. The variance was slightly higher and the response time was longer for Cylinder 1.

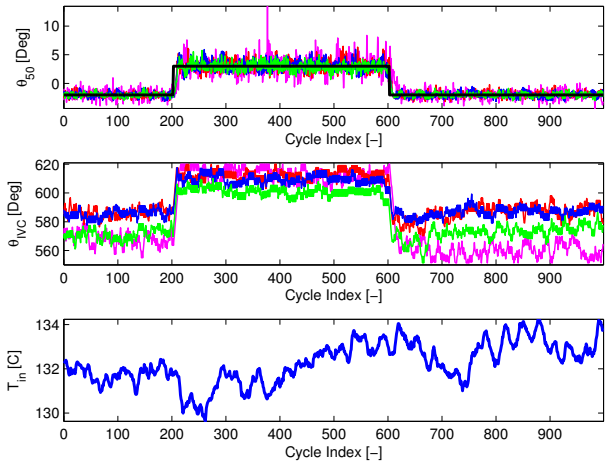

Fig. 9. Response to step changes in the set-point for θ_{50} for cylinders 1, 3, 5, and 6. The controller for cylinder 5 governed the intake temperature.

VI. Discussion

A midranging intake temperature control strategy was chosen and manually tuned. It is possible that a model-based control design could improve the closed-loop performance. Combined with estimation of the flows past the valves this would also extend the operating range as smaller values of α_{HV} would be admissible without risking damages to the heater. The non-zero lower bound on α_{HV} could be replaced by setting $q_h = 0$ when α_{HV} goes below a threshold. The intake temperature control could also be included in the top-level predictive controller.

The closed-loop system had a fairly short response time. For step changes in θ_{50} of a few degrees around the linearization point the response time was approximately ten cycles. Only the larger steps (e.g., from -2 to 4 and from 4 to -3 in Fig. 6) took around 15 cycles, which compares well with previously published results [8], [1]. The inlet valve closing showed to be a sufficient control signal in many operating points. The need for an additional control signal to extend the operating range is, however, apparent e.g. in the end of Fig. 6 and during the EGR-disturbance in Fig. 8.

The output variance under closed-loop control increased with later combustion phasing (Fig. 7). As the variance could be reduced either by introducing a disturbance model or by using a linearization made closer to the operating point, the cause seems to be a combination of physical effects and model errors. The closed-loop system showed good robustness to disturbances in engine speed, fuel amount, and EGR level. The EGR seems to have the greatest impact on θ_{50} and there was a clear transient occurring in response to the increase. A likely cause is that the thermal properties of the charge are altered by increasing the amount of residuals. Also, as seen in Fig. 8, the change in EGR is not reflected in IMEP_n, which is used as measurement in the controller. Whereas the initial multi-cylinder control results are good, there was a fairly wide spread in the required θ_{IVC} (Fig. 9). The situation is similar to that in [14] where a long-route EGR-system was used together with VVA. Both the long-route EGR level and the intake temperature are global variables shared by all cylinders [14].

VII. Conclusion

Model predictive control of the combustion phasing in an HCCI engine using a physical model was investigated. To obtain fast control of the intake temperature, Fast Thermal Management was implemented using mid-ranging control. The physical model included cylinder wall temperature dynamics, giving a physically reasonable explanation for the cycle-to-cycle dynamics when only small amounts of hot residuals were trapped in the cylinder. The robustness of the controller was investigated by introducing disturbances in the engine speed, the amount of fuel, and the amount of cooled recycled exhaust gases. A disturbance model was included in the controller, yielding a decrease in the steady-state variance. A comparable decrease was, however, achieved by using a linearization performed closer to the operating point, showing the advantage of physically motivated models. The effects of changing prediction and control horizons in the controller were investigated both in terms of performance and computation time. The results suggest that fairly short control- and prediction horizons are sufficient.

VIII. Acknowledgements

The authors are grateful for technical discussion and co-operation with M. Karlsson. This research was supported by KCFP, Closed-Loop Combustion Control (Swedish Energy Adm: Project no. 22485-1) and by Vinnova and Volvo Powertrain Corporation.

References

[1] J. Bengtsson, P. Strandh, R. Johansson, P. Tunestål, and B. Johansson, "Hybrid modelling of homogeneous charge compression ignition (HCCI) engine dynamic—A survey," *Int. J. Control*, vol. 80, no. 11, pp. 1814–1848, Nov. 2007.

[2] J. Maciejowski, *Predictive Control with Constraints*. Essex, England: Prentice-Hall, 2002.

[3] A. Widd, P. Tunestål, C. Wilhelmsson, and R. Johansson, "Control-oriented modeling of homogeneous charge compression ignition incorporating cylinder wall temperature dynamics," in *Proc. 9th Int. Symp. Advanced Vehicle Control*, Kobe, Japan, Oct. 2008.

[4] A. Widd, P. Tunestål, and R. Johansson, "Physical modeling and control of homogeneous charge compression ignition (HCCI) engines," in *Proc. 47th IEEE Conf. Decision and Control*, Cancun, Mexico, Dec. 2008, pp. 5615-5620.

[5] C.-J. Chiang, A. G. Stefanopoulou, and M. Jankovic, "Nonlinear observer-based control of load transitions in homogeneous charge compression ignition engines," *IEEE Trans. Control Systems Technology*, vol. 15, no. 3, pp. 438–448, 2007.

[6] G. M. Shaver, M. Roelle, and J. C. Gerdes, "A two-input two-output control model of HCCI engines," in *Proc. 2006 Am. Control Conf.*, Minneapolis, MN, USA, June 2006.

[7] M. J. Roelle, N. Ravi, A. F. Jungkunz, and J. C. Gerdes, "A dynamic model of recompression HCCI combustion including cylinder wall temperature," in *Proc. IMECE2006*, Chicago, Illinois, USA, Nov. 2006.

[8] D. Blom, M. Karlsson, K. Ekholm, P. Tunestål, and R. Johansson, "HCCI engine modeling and control using conservation principles," *SAE Technical Papers*, no. 2008-01-0789, 2008.

[9] G. Haraldsson, "Closed-loop combustion control of a multi cylinder HCCI engine using variable compression ratio and fast thermal management," Ph.D. dissertation, TMPH–05/1028, Dept. Heat and Power Engineering, Lund University, Sweden, Jan. 2005.

[10] J. Bengtsson, "Closed-loop control of HCCI engine dynamics," Ph.D. dissertation, TFRT–1070, Dept. Automatic Control, Lund University, Sweden, Nov. 2004.

[11] J. B. Heywood, *Internal Combustion Engine Fundamentals*. New York: McGraw-Hill, 1988.

[12] C. Chiang and A. Stefanopoulou, "Sensitivity analysis of combustion timing and duration of homogeneous charge compression ignition (HCCI) engines," in *Proc. 2006 Am. Control Conf.*, Minneapolis, MN, USA, June 2006.

[13] B. J. Allison and A. J. Isaksson, "Design and performance of mid-ranging controllers," *J. Process Control*, vol. 8, no. 5-6, pp. 469–474, 1998.

[14] M. Karlsson, K. Ekholm, P. Strandh, R. Johansson, P. Tunestål, and B. Johansson, "Closed-loop control of combustion phasing in an HCCI engine using VVA and variable EGR," in *Fifth IFAC Symp. Adv. Automotive Control*, Monterey, USA, Aug. 2007.

[15] J. Bengtsson, P. Strandh, R. Johansson, P. Tunestål, and B. Johansson, "Model predictive control of homogeneous charge compression ignition (HCCI) engine dynamics," in *2006 IEEE Int. Conf. Control Appl.*, Munich, Germany, Oct. 2006, pp. 1675-1680.

[16] J. Åkesson and P. Hagander, "Integral action – A disturbance observer approach," in *Proc. Eur. Control Conf.*, Cambridge, UK, Sept. 2003.

[17] P. Strandh, "HCCI operation - closed loop combustion control using vva or dual fuel," Ph.D. dissertation, TMPH–06/1039, Dept. Energy Sciences, Lund University, Sweden, May 2006.

[18] R. Johansson, *System Modeling and Identification*. Englewood Cliffs, NJ: Prentice Hall, 1993.